Personalised gravitational loading of the cervical spine from biplanar X-rays for asymptomatic and clinical subjects in neutral standing position

Christophe Muth-seng [a,*], Maxime Huneidi [b], Cécile Heidsieck [a], Sébastien Laporte [a], Jean-Yves Le Coz [a], Olivier Gille [b], Wafa Skalli [a]

[a] Arts et Métiers Institute of Technology, Université Sorbonne Paris Nord, IBHGC - Institut de Biomécanique Humaine Georges Charpak, HESAM Université, F-75013, Paris, France

[b] Service de chirurgie orthopédique et traumatologique, Groupe Hospitalier Pellegrin, CHU de Bordeaux, Bordeaux 33076, France

Keywords:
Cervical spine
Gravitational loading
Subject-specific
Standing position

ABSTRACT

Background: As a leading cause of disability with a high societal and economic cost, it is crucial to better understand risk factors of neck pain and surgical complications. Getting subject-specific external loading is essential for quantifying muscle forces and joint loads but it requires exertion trials and load cells which are uncommon in clinical settings.

Methods: This paper presents a method to compute the gravitational loading at four levels of the cervical spine (C3C4, C4C5, C5C6, C6C7) in neutral standing position from biplanar radiographs exclusively. The resulting load was decomposed in local disc frames and its components were used to compare different populations: 118 asymptomatic subjects and 46 patients before and after surgery (anterior cervical discectomy and fusion or total disc replacement). Comparisons were performed at C6C7 and the upper level adjacent to surgery.

Findings: Significant changes in gravitational loading were observed with age in healthy subjects as well as in patients after surgery and have been associated with changes in posture.

Interpretation: This approach quantifies the influence of postural changes on gravitational loading on the cervical spine. It represents a simple way to obtain necessary input for muscle force quantification models in clinical routine and to use them for patient evaluation. The study of the subsequent subject-specific spinal loading could help further the understanding of cervical spine biomechanics, degeneration mechanisms and complications following surgery.

1. Introduction

Neck pain has been identified as one of the three most common musculoskeletal disorders (Trinh et al., 2006) and as the fourth leading cause for disability in the US (Murray et al., 2013). Its annual prevalence has been reported to range between 15 and 50% (Binder, 2008; Fejer et al., 2006; Fernández-De-Las-Peñas et al., 2011; Hogg-Johnson et al., 2009) and, with the soaring ubiquity of portable electronics and changes in lifestyle, is expected to keep rising (Côté et al., 2008; Vasavada et al., 2015). It entails major societal and economic expenses in both direct (Dieleman et al., 2016) and indirect costs (Côté et al., 2009).

Surgery as a treatment to alleviate neck pain has been on a rising trend (Marquez-Lara et al., 2014; Wang et al., 2009). While anterior cervical discectomy and fusion (ACDF) appears to be the gold standard, total disc replacement (TDR) has become a motion-preserving alternative. Complications following surgery, such as adjacent segment disease (ASD), have been reported for both though (Bevevino and Hilibrand, 2016; Bible and Kang, 2016; Kong et al., 2016).

The burden neck pain represents to patients' quality of life and expenses makes it crucial to further prevention. Though some risk factors have been identified, including muscular dysfunction (Alpayci et al., 2016; Cheng et al., 2014; Falla et al., 2007; Fernández-de-las-Peñas et al., 2008) and sagittal posture (Lau et al., 2010) for neck pain and spine curvature for ASD (Katsuura et al., 2001; Xiong et al., 2020), a deeper understanding of cervical spine biomechanics and degeneration is still needed.

Numerical modelling can be a precious tool in that regard for assessing the influence of geometry, loading, for implant design and patient evaluation. While advancements have been made towards personalised geometry (John et al., 2019; Laville et al., 2009; Nikkhoo

Corresponding author at: Institut de Biomécanique Humaine Georges Charpak, Arts et Métiers, 151 Boulevard de l'Hôpital, 75013 Paris, France.
E-mail address: christophe.muth-seng@ensam.eu (C. Muth-seng).

et al., 2019) and numerical implant evaluation (Gandhi et al., 2019; Mackiewicz et al., 2016; Rousseau et al., 2008), obtaining subject-specific loading remains challenging. Musculoskeletal models can actually yield personalised spinal loading but they require exertion trials including external loading and other measurements, such as motion capture and EMG (Alizadeh et al., 2020; Moroney et al., 1988; Mortensen et al., 2018). This experimental pre-requisite makes them difficult to implement into a clinical setting.

Recent developments of low-dose biplanar X-ray full-body acquisitions (Dubousset et al., 2010) in standing position with associated 3D reconstructions (Humbert et al., 2009; Nérot et al., 2015; Rousseau et al., 2007) allows subject-specific postural analysis in clinical routine. Particularly, reconstruction of the external envelope associated with density models allows an estimation of mass and the centre of mass of each body segment (Amabile et al., 2016). Computation of the barycentre of the body segment above a given joint allows estimation of the gravitational load taking into account subject-specific posture (Amabile et al., 2015). The clinical relevance of this barycentremetric approach has been assessed in the study of idiopathic scoliosis (Thenard et al., 2019).

Using a similar approach, the present study deals with obtaining subject-specific gravitational loading of the cervical spine from biplanar X-rays for both asymptomatic and clinical subjects. Decomposition of the resulting load should help quantify significant differences between age groups and between healthy/clinical subjects, providing insight regarding the mechanical effects of age, pathology and treatment.

2. Methods

2.1. Populations

The control population was constituted from data of 118 healthy subjects (57 females, 61 males) of mean age 42.0 y.o. (SD: 11.5) acquired during previous studies (Heidsieck et al., 2021). Clinical exams were performed to ensure that the subjects presented no symptomatic lower limb nor spine pathology that could affect the spinal alignment and patient with a frontal Cobb angle over 20° were excluded.

The clinical population was made up of 46 patients (29 females, 16 males) of mean age 51.4 y.o. (SD: 11.5) experiencing neck pain and treated by surgery. Thirteen underwent TDR, including four with a CP-ESP prosthesis (FH Orthopedics) and nine using a Baguera prosthesis (SpineArt SA, Geneva, Switzerland), and the remaining 33 underwent ACDF. Their data were collected pre and post-surgery (follow-up ranged from 6 weeks to 2 months) in routine clinical practice.

Data acquisition was performed after subjects' written consent and approval by an ethics committee (Comité de Protection des Personnes CPP N° 2010/113, N° 06036 for control population, and N° 2014/89 for patients).

Populations under study were sorted into three age groups: younger than 40 y.o, between 40 and 60 y.o. and over 60 y.o., which will be referred to as G1, G2 and G3 respectively. Further details on the populations are available in Table 1.

2.2. 3D reconstructions and barycentremetry

Each subject underwent biplanar X-rays in free standing position (Steffen et al., 2010) acquired using an EOS system (EOS imaging SA., Paris, France). This allowed 3D reconstructions of the spine from C1 to L5 (Humbert et al., 2009; Rousseau et al., 2007) and of the body envelope from head to toe using a validated semi-automatic method (Nérot et al., 2015), briefly reminded hereafter. Manual positioning of a few anatomical landmarks allowed morphing of a reference average template (either male or female). The resulting initial model was then retroprojected on each X-Rays and manually adjusted to fit the subject's contours.

From the 3D model of the spine, a plane was assessed at four intervertebral disc (IVD) levels (C3C4, C4C5, C5C6, C6C7) using the adjacent endplates, and a local frame was computed for each based on the vertebral frames as defined by Rousseau et al. (2007). Details of the method and the evaluation of its reproducibility are available in Supplementary Data.

The IVD planes were used to intersect the model of the body envelope. For each of them, the volume of everything above it was computed. Combined with a generic uniform density model for the head and neck (Dempster and Gaughran, 1967), body segment mass and barycentre were estimated; yielding the mechanical loading on each IVD due to gravity (Fig. 1a).

Said gravitational loading was decomposed from the local IVD frame (Fig. 1b) into force components: posteroanterior shear (Fx), mediolateral shear (Fy) and compression (Fz) and moment components: mediolateral (Mx), flexion-extension (My) and axial torsion (Mz). Posteroanterior and mediolateral moment arms from the disc centre to the centre of mass were measured, as well as the disc tilt angle with regards to the horizontal plane.

A reproducibility study (20 subjects, 2 operators, 2 times per operator) yielded standard deviations of uncertainty on IVD plane orientation of 1.3°, 1.6° and 1.5° in the frontal, sagittal and axial planes respectively. These uncertainties were used as random errors in a Monte-Carlo analysis repeated 2000 times for a healthy subject to quantify its impact on the components of the gravitational force.

2.3. Analysis and statistical tests

A linear correlation study was carried out for the asymptomatic populations to assess the influence of age, weight and height on head-neck mass, C6C7 disc angulation and posteroanterior and mediolateral moment arms to the disc centre.

Statistical tests were performed for each component of mechanical

Table 1
Control and clinical populations.

Level	Age group	Posteroanterior shear Fx (N)	Mediolateral shear Fy (N)	Compression Fz (N)	Flexion-Extension moment My (Nm)
	< 40 y.o.	18,5 (5,3)	−1,5 (3,0)	−37,9 (4,3)	0,67 (0,46)
C3C4	40–60 y.o.	18,0 (4,3)	−1,1 (3,4)	−39,5 (7,6)	0,47 (0,39)
	> 60 y.o.	19,2 (6,5)	−2,1 (3,7)	−37,1 (4,9)	0,66 (0,56)
	< 40 y.o.	18,1 (5,5)	−1,8 (3,5)	−40,4 (5,4)	0,84 (0,51)
C4C5	40–60 y.o.	18,5 (7,1)	−1,6 (3,9)	−41,0 (11)	0,61 (0,49)
	> 60 y.o.	20,0 (6,8)	−2,5 (3,5)	−38,8 (4,8)	0,83 (0,66)
	< 40 y.o.	**17,2 (6,1)***	−2,1 (3,6)	**−43,0 (4,7)***	0,97 (0,58)
C5C6	40–60 y.o.	20,0 (7,5)	−1,7 (4,2)	−42,6 (9,2)	0,78 (0,54)
	> 60 y.o.	**22,8 (7,3)***	−3,0 (3,4)	**−39,1 (5,4)***	1,0 (0,74)
	< 40 y.o.	**16,2 (6,8)*,****	−2,4 (3,6)	**−45,5 (4,7)***	1,1 (0,65)
C6C7	40–60 y.o.	**20,5 (8,3)****	−2,3 (4,2)	−44,8 (9)	1,0 (0,64)
	> 60 y.o.	**23,4 (7,1)***	−3,0 (3,2)	**−41,2 (5,7)***	1,3 (0,84)

Numbers in bold indicate the significantly different groups, with associated p values: *$0.02 \leq p \leq 0.05$ **$p \leq 0.005$.

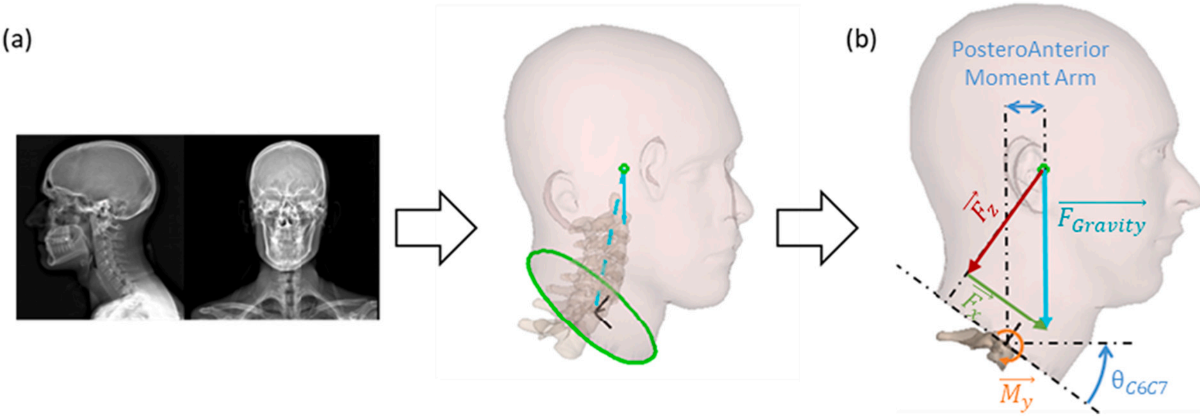

Fig. 1. (a) 3D reconstruction of the spine and body envelope from stereoradiographs (b) Sagittal illustration of the decomposition of the gravity force in the local C6C7 IVD frame.

loading at the C6C7 level to compare groups G1, G2, G3 of the asymptomatic population; as well as between the G2 groups of the control and clinical populations pre and post-surgery. Distribution normality was evaluated using a Shapiro-Wilk test. Then, comparisons between groups were made via either ANOVA or Kruskal-Wallis test (depending on normality) followed by a post hoc analysis using the Tukey-Kramer method. Additionally, paired comparisons for each components at C6C7 between pre and post-surgery were performed using either paired *t*-tests or Wilcoxon signed-rank tests (depending on normality).

Finally, at each IVD level, normality and subnormality corridors were defined for each component based on the means and standard deviations (SD) from each group of the control population (median and interquartile range for non-normal distributions). Patients' results were considered normal if they were less than 1*SD away from the control mean value, subnormal if less than 2*SD away, and abnormal beyond. This analysis was performed at the C6C7 IVD and at the level upper-adjacent to the operated IVD.

Every significant difference and observation on load components from either statistical or corridor analysis was complemented with a similar analysis comparing moment arms and IVD tilt angle.

3. Results

Reconstruction of the cervical spine and the body envelope took 15 to 20 min per subject, and the associated loading was computed in a matter of seconds. Following the sensitivity analysis, the uncertainty on the C6C7 disc plane orientation yielded 95% confidence intervals lesser than 0.1 N for all three force components projected from the body segment weight.

As results regarding mediolateral and torsion moments were less than 0.5 Nm and that the associated analyses showed no significant difference between groups, the following results will focus on the other components.

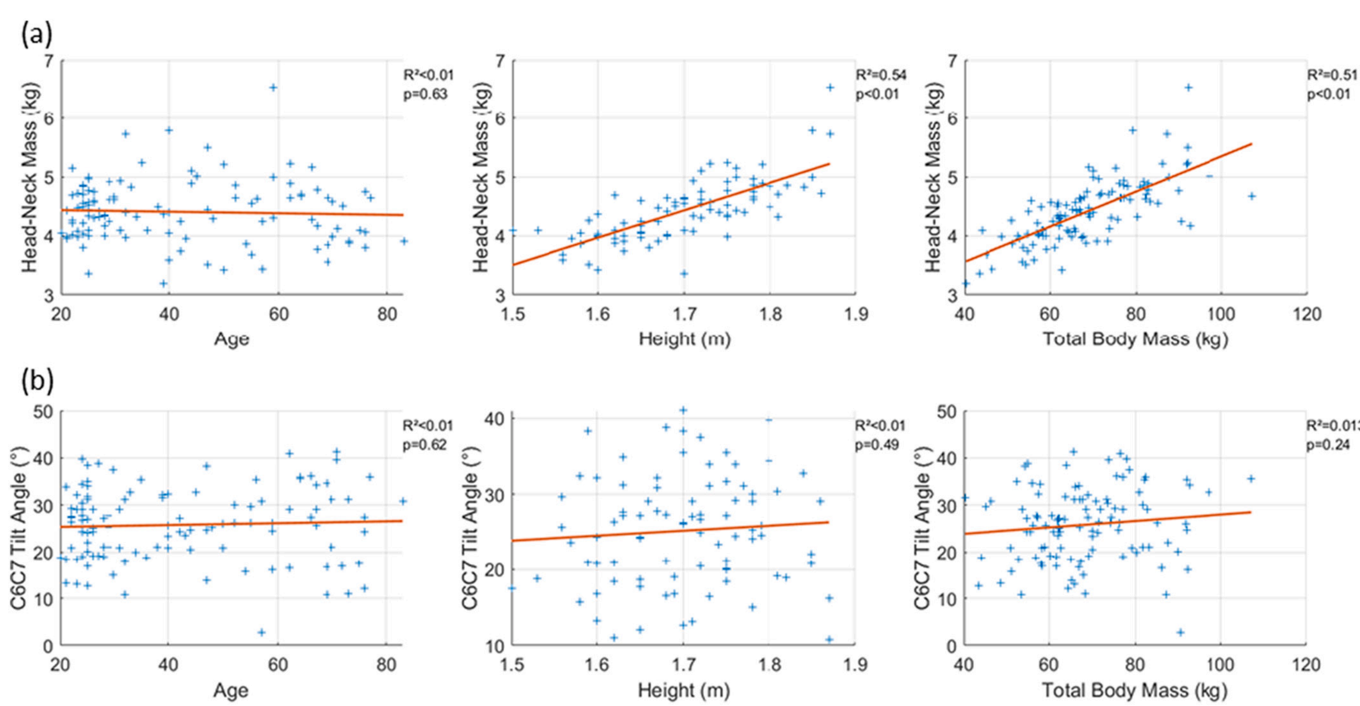

Fig. 2. Correlation study of the head-neck mass (a) and the C6C7 tilt angle (b) with subjects' age, height and total body mass. Tilt angle is measured positive clockwise to horizontal, illustrated as θ_{C6C7} in Fig. 1b.

3.1. Comparing asymptomatic subjects

Average mass of the head-neck segment above C6C7 of healthy subjects was 5.0 (SD: 0.7) kg. It was correlated with subjects' height ($R^2 = 0.59$, $p = 8.3\ 10^{-8}$) and total body mass ($R^2 = 0.57$, $p = 2.5\ 10^{-21}$), but not age (Fig. 2a). Regarding C6C7 sagittal tilt angle, only a low correlation with subject's age was found ($R^2 = 0.2$, $p = 5.7\ 10^{-7}$) (Fig. 2b). G1 had a significantly lower sagittal tilt than G2 and G3 ($p = 0.028$ and $2.5\ 10^{-6}$ respectively.) Average tilt angles were 19.5° (SD: 7.7), 24.4° (SD: 8.3) and 29.6° (SD: 8.8) for G1, G2 and G3 respectively. Posteroanterior and mediolateral moment arms were not correlated to age, total mass or height, and were on average of 23 (SD: 14) mm and 2.7 (SD: 8) mm respectively.

All components of the loading at C6C7 were normally distributed for the control G1 and G3 groups. For the control G2 group, only the compression and mediolateral moment components were not normally distributed ($p = 0.03$ and 0.04 respectively). Variance analysis (Fig. 3) showed that control G1 had significantly lower posteroanterior shear than control G2 and G3 ($p = 0.034$ and $7.32 \cdot 10^{-4}$ respectively) as well as significantly higher compression than control G3 ($p = 0.006$).

The mean and SD values of each component at each IVD, which were instrumental in defining normality corridors, are available in Table 2.

3.2. Comparing control, pre and post-surgery

3.2.1. Statistical analysis at C6C7 for subjects between 40 and 60 y.o

Components of C6C7 loading for control-G2 were normally distributed except in compression ($p = 0.031$), mediolateral moment ($p = 0.039$) and in torsion ($p = 0.35$). For preoperative-G2, only the flexion-extension moment was not ($p = 0.067$). Finally, for postoperative-G2 only the compression ($p = 0.010$) and torsion ($p = 0.0031$) components were not normally distributed.

Group comparisons (Fig. 4) found mediolateral shear was significantly closer to zero in the preoperative than in the control group ($p = 0.026$). This observation was confirmed by a significantly higher frontal tilt angle for control than for preop subjects ($p = 0.022$). Furthermore, the paired analysis highlighted a significantly lower posteroanterior shear ($p = 1.31 \cdot 10^{-4}$) before surgery than after. Similarly, preoperative sagittal tilt angle was found significantly lower than post-surgery ($p = 4.53 \cdot 10^{-5}$).

Table 2
Mean (SD) values of each component of the gravitational load for asymptomatic subjects of different age groups at each IVD level.

	Control	Clinical					
Age group	$N_{subjects}$	$N_{subjects}$	Surgery	Surgery level			
				C3C4	C4C5	C5C6	C6C7
G1 < 40 y.o.	65	5	1 ACDF			1	
			4 TDR			2	2
G2 40–60 y.o.	27	33	24 ACDF	1	3	13	7
			9 TDR			4	5
G3 > 60 y.o.	26	8	8 ACDF			6	2
			0 TDR				

ACDF: Anterior Cervical Discectomy and Fusion; TDR: Total Disc Replacement.

3.2.2. Corridor analysis

Table 3 shows the evolution of the number of clinical subjects with weight components within the normality and subnormality corridors in pre and postoperative at C6C7 and at the level upper-adjacent to the surgery.

At C6C7, except in mediolateral shear, consistently more subjects were considered normal after surgery. Similarly, regarding individual patients changing corridors, up to three more of them got closer to normality than those that got further from it for posteroanterior shear, compression and flexion-moment.

At the upper level adjacent to the operation, a few more subjects got further from normality regarding effort components. Regarding the flexion-extension moment, 14 subjects (30% of the population) changed corridors towards normality, over three times as many as those that got further away from it. Anteroposterior moment arm of that level followed the same trend, with 13 subjects getting closer to normality.

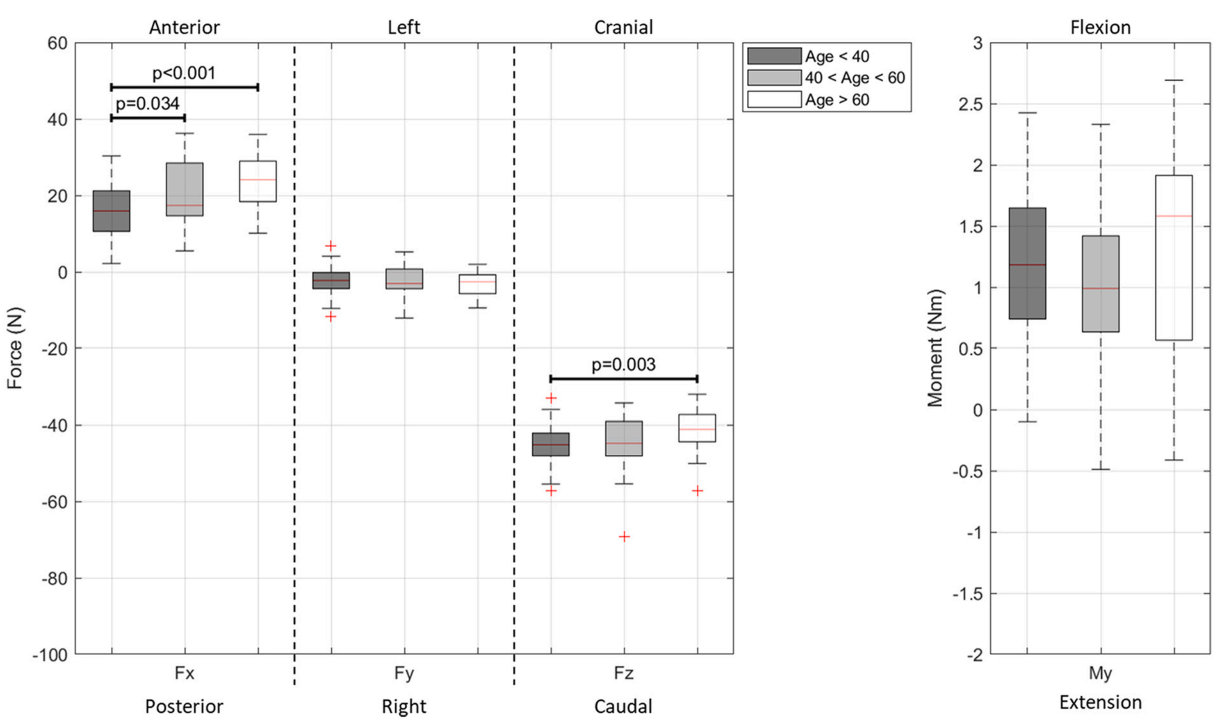

Fig. 3. Distribution of the components of the gravitational loading at C6C7 for asymptomatic subjects. Shear and compression components are on the left-hand side, flexion-extension moment component on the right-hand side. Horizontal bars indicate significant differences.

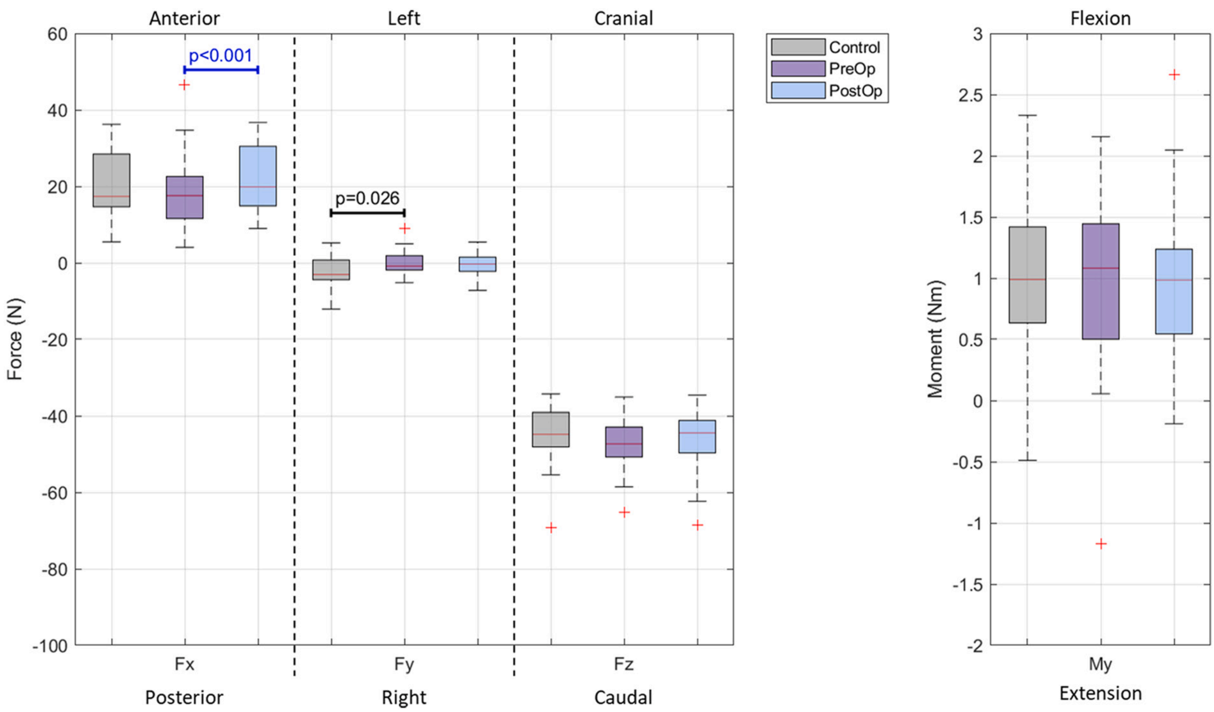

Fig. 4. Distribution of the components of the gravitational loading at C6C7 for asymptomatic, pre and postoperative subjects. Shear and compression components are on the left-hand side, flexion-extension moment component on the right-hand side. Black and blue horizontal bars indicate significant differences from variance and paired analysis respectively. (For interpretation of the references to colour in this figure legend, the reader is referred to the web version of this article.)

Table 3
Evolution of the gravitational load components following surgery with regards to the corridors from control subjects at C6C7 and at the level upper-adjacent to the operated IVD.

		Posteroanterior shear Fx (N)			Mediolateral shear Fy (N)			Compression Fz (N)			Flexion-Extension moment My (Nm)		
C6C7		N_{norm}	N_{sub}	N_a	N_{norm}	N_{sub}	N_a	N_{norm}	N_{sub}	N_a	N_{norm}	N_{sub}	N_a
	PreOp	25	20	1	35	9	2	34	9	3	29	13	1
	PostOp	27	18	1	32	14	0	36	7	3	32	16	1
	Evolution	$N^+ = 10$ $N^- = 8$			$N^+ = 5$ $N^- = 7$			$N^+ = 3$ $N^- = 1$			$N^+ = 10$ $N^- = 7$		
Upper-adjacent		N_{norm}	N_{sub}	N_a	N_{norm}	N_{sub}	N_a	N_{norm}	N_{sub}	N_a	N_{norm}	N_{sub}	N_a
	PreOp	26	14	5	36	8	1	35	9	1	25	19	1
	PostOp	24	18	3	34	10	1	33	11	1	37	6	2
	Evolution	$N^+ = 8$ $N^- = 9$			$N^+ = 5$ $N^- = 7$			$N^+ = 5$ $N^- = 6$			$N^+ = 14$ $N^- = 4$		

N_{norm}, N_{sub} and N_a correspond to numbers of subjects that are considered normal, subnormal or abnormal respectively.
N^+ (respectively N^-) correspond to number of subjects changing corridor by getting closer (respectively further) to the mean value of the control group.

4. Discussion

This present work aimed at developing a method to compute personalised mechanical loading of the cervical spine from medical images. From biplanar radiographs, the mass of the head-neck segment, moment arms and gravitational loading in standing position were quantified at multiple IVD levels for both asymptomatic and clinical subjects pre and postoperative. The method used was fast, only required medical images and reconstruction time could be cut down further using automation (Gajny et al., 2019). The robustness of the method was verified with respect to the uncertainties associated with spine reconstruction.

While the presented approach yields subject-specific gravitational loadings of the cervical spine in neutral standing position, as it does not account for muscular response, it provides an incomplete spinal loading. For instance, though the external compression from this barycentremetric approach may correspond to 75% of the actual intervertebral joint compression assessed with a proprioception-based muscle model (Van den Abbeele et al., 2018), it appears to represent less than 50% of the joint compression from other models (Barrett et al., 2020; Bayoglu et al., 2019; Moroney et al., 1988). As such, the resulting loading from the present method should be used as input to employ muscle force quantification models.

4.1. Asymptomatic subjects

The mass of the head-neck segment of asymptomatic subjects above the C6C7 disc level estimated in this study are consistent with the values reported in the literature (Clauser et al., 1969; Dempster and Gaughran, 1967; Yoganandan et al., 2009). Its correlation with subject weight and height could be explained by the slight increase in segment volume related to these two variables.

Correlation and statistical analyses showed a significant increase of the tilt angle of C6C7, i.e. the IVD becomes more vertical, with age. This observation is consistent with studies on the effect of age on cervical alignment in asymptomatic subjects, reporting changes in lordosis (Gore et al., 1986; Klinich et al., 2004; Liu et al., 2019) and an increase in thoracic kyphosis (Boyle et al., 2002). Cervical spine tissue degeneration is also very common, with up to 81% of healthy subjects showing signs of it within 10 years (Okada et al., 2009) without experiencing symptoms, and has been associated with postural changes (Gore et al., 1986). No such observation could be made regarding the moment arms.

The present study quantifies the influence of this change in alignment on the gravitational loading of C6C7 and shows a significant increase in posterior-anterior shear and a significant decrease in compression between G1 and G3. This observation reflects C6C7 becoming more vertical with age, which tends to align the local posterior-anterior direction of the IVD with that of gravity. Though the increase in shear may be rather small - from 16.2 (SD 6.8) N to 23.4 (SD 7.1) N – it may indicate a less economical posture for aging subjects, requiring a higher muscular response and making them more susceptible to fatigue.

4.2. Control and clinical subjects

Statistical comparisons performed for subjects between 40 and 60 y.o. mainly revealed a significant difference between asymptomatic and preoperative subjects in mediolateral shear stress at C6C7. This difference was not apparent for postoperative patients, which was consistent with the frontal tilt of the disc getting closer to control values after surgery. The paired analysis showed the C6C7 became significantly more vertical, thus significantly increasing the posterior-anterior shear component between pre and postoperative. Studying the evolution of patients with regards to the normality corridors from the control group mainly showed improvement for the flexion-extension moment at the IVD upper-adjacent to the operated level, stemming from a change in gravitational moment arm.

However, these observations are limited by the absence of evaluation of the evolution of pain for the patients, as well as by the very short postoperative follow-up. Studies with much longer postoperative follow-ups have demonstrated changes in cervical alignment in both arthrodesis (Hyun et al., 2017; Lan et al., 2019) and arthroplasty (Guérin et al., 2012; Kim et al., 2008; Wang et al., 2021). Some of these changes have been identified as risk factors for complications such as ASD (Katsuura et al., 2001; Xiong et al., 2020) and pseudarthrosis (Choi et al., 2017).

Another limitation of this study is the small number of patients. Although there were 33 patients treated with arthrodesis, only a dozen underwent an arthroplasty. Further longitudinal studies performed on a larger population could investigate the gravitational loads not only at the upper adjacent level but also at the operated and lower adjacent level, both for non fusion and for fusion techniques. This would increase our understanding on how gravitational forces analysis, in relation with subject specific posture, can impact the clinical outcome.

5. Conclusion

In this article was described a method to obtain personalised external loading of the cervical spine in neutral standing position and its decomposition in local IVD frames using biplanar X-rays exclusively. Comparisons between populations yielded significantly different loadings among asymptomatic subjects as well as pre and postoperative patients in posterior-anterior shear and compression. The present method should be easier to implement in a clinical setting than exertion trials and provide necessary inputs to muscle force quantification models and actual joint load assessment for patient evaluation.

Declaration of Competing Interest

None declared.

Acknowledgements

The authors would like to express their gratitude to the BiomecAM chair program of Fondation ParisTech, financed by Société Générale, Covea, Proteor and Fondation Cotrel, who supported and funded this study. They would also like to thank the staff of Hôpital Pellegrin (Bordeaux) and Hôpital privé Francheville (Périgueux) for their contribution to clinical data acquisition.

Appendix A. Supplementary data

Supplementary data to this article can be found online at https://doi.org/10.1016/j.clinbiomech.2022.105577.

References

Alizadeh, M., Aurand, A., Knapik, G.G., Dufour, J.S., Mendel, E., Bourekas, E., Marras, W. S., 2020. An electromyography-assisted biomechanical cervical spine model: model development and validation. Clin. Biomech. 80, 105169.

Alpayci, M., Şenköy, E., Delen, V., Şah, V., Yazmalar, L., Erden, M., Toprak, M., Kaplan, Ş., 2016. Decreased neck muscle strength in patients with the loss of cervical lordosis. Clin. Biomech. 33, 98–102.

Amabile, C., Nérot, A., Choisne, J., Pillet, H., Lafage, V., Skalli, W., 2015. Alignment of centers of mass of body segments with the gravity line. Comput. Methods Biomech. Biomed. Engin. 18 (August), 1870–1871.

Amabile, C., Choisne, J., Nérot, A., Pillet, H., Skalli, W., 2016. Determination of a new uniform thorax density representative of the living population from 3D external body shape modeling. J. Biomech. [Internet]. 49 (7), 1162–1169. https://doi.org/10.1016/j.jbiomech.2016.03.006.

Barrett, J.M., McKinnon, C., Callaghan, J.P., 2020. Cervical spine joint loading with neck flexion. Ergonomics [Internet]. 63 (1), 101–108. https://doi.org/10.1080/00140139.2019.1677944.

Bayoglu, R., Galibarov, P.E., Verdonschot, N., Koopman, B., Homminga, J., 2019. Twente spine model: a thorough investigation of the spinal loads in a complete and coherent musculoskeletal model of the human spine. Med. Eng. Phys. [Internet]. 68, 35–45. https://doi.org/10.1016/j.medengphy.2019.03.015.

Bevevino, A.J., Hilibrand, A.S., 2016. Adjacent segment disease: incidence and recommended treatment. Semin Spine Surg. 28 (2), 107–114.

Bible, J.E., Kang, J.D., 2016. Anterior cervical discectomy and fusion: surgical indications and outcomes. Semin Spine Surg. 28, 80–83.

Binder, A., 2008. Musculoskeletal disorders neck pain search date may 2007 musculoskeletal disorders neck pain. Clin. Evid. (Online). 08 (1103), 1–34.

Boyle, J.J.W., Milne, N., Singer, K.P., 2002. Influence of age on cervicothoracic spinal curvature: an ex vivo radiographic survey. Clin. Biomech. 17 (17), 361–367.

Cheng, C.-H., Cheng K., H.-Y., Chen P.-C., C., Lin, K.-H., Liu, W.-Y., Wang, S.-F., Hsu, W.-L., Chuang, Y.-F., 2014. Altered co-contraction of cervical muscles in Young adults with chronic neck pain during voluntary neck motions. J. Phys. Ther. Sci. 26 (4), 587–590. https://doi.org/10.1589/jpts.26.587.

Choi, S.H., Cho, J.H., Hwang, C.J., Lee, C.S., Gwak, H.W., Lee, D.H., 2017. Preoperative radiographic parameters to predict a higher pseudarthrosis rate after anterior cervical discectomy and fusion. Spine (Phila Pa 1976) 42 (23), 1772–1778.

Clauser, C.E., McConville, J.T., Young, J.W., 1969. Weight, Volume, and Center of Mass of Segments of the Human Body. Springfield.

Côté, P., Carroll, L.J., Carragee, E.J., Nordin, M., Guzman, J., van der Velde, G., Cassidy, J.D., Carroll, L.J., Hogg-Johnson, S., Holm, L.W., et al., 2008. The burden and determinants of neck pain in workers. Spine (Phila Pa 1976) 33 (Suppl. 1), S60–S74.

Côté, P., Kristman, V., Vidmar, M., Van Eerd, D., Hogg-Johnson, S., Beaton, D., Smith, P. M., 2009. The prevalence and incidence of work absenteeism involving neck pain. A cohort of ontario lost-time claimants. J. Manipulative Physiol. Ther. 32 (2 SUPPL), S219–S226.

Dempster, W.T., Gaughran, G.R.L., 1967. Properties of body segments based on size and weight. Am. J. Anat. 120 (1), 33–54.

Dieleman, J.L., Baral, R., Birger, M., Bui, A.L., Bulchis, A., Chapin, A., Hamavid, H., Horst, C., Johnson, E.K., Joseph, J., et al., 2016. US spending on personal health care and public health, 1996-2013. JAMA - J. Am. Med. Assoc. 316 (24), 2627–2646.

Dubousset, J., Charpak, G., Skalli, W., Deguise, J., Kalifa, G., 2010. EOS: a new imaging system with low dose radiation in standing position for spine and bone; joint disorders. J. Musculoskelet. Res. 13 (01), 1–12.

Falla, D., Farina, D., Dahl, M.K., Graven-Nielsen, T., Kanstrup Dahl, M., Graven-Nielsen, T., 2007. Muscle pain induces task-dependent changes in cervical agonist/antagonist activity. J. Appl. Physiol. 102 (2), 601–609.

Fejer, R., Kyvik, K.O., Hartvigsen, J., 2006. The prevalence of neck pain in the world population: a systematic critical review of the literature. Eur. Spine J. 15 (6), 834–848.

Fernández-de-las-Peñas, C., Falla, D., Arendt-Nielsen, L., Farina, D., 2008. Cervical muscle co-activation in isometric contractions is enhanced in chronic tension-type headache patients. Cephalalgia. 28 (7), 744–751.

Fernández-De-Las-Peñas, C., Hernández-Barrera, V., Alonso-Blanco, C., Palacios-Ceña, D., Carrasco-Garrido, P., Jiménez-Sánchez, S., Jiménez-García, R., 2011. Prevalence of neck and low back pain in community-dwelling adults in spain: A population-based national study. Spine (Phila Pa 1976) 36 (3).

Gajny, L., Ebrahimi, S., Vergari, C., Angelini, E., Skalli, W., 2019. Quasi-automatic 3D reconstruction of the full spine from low-dose biplanar X-rays based on statistical inferences and image analysis. Eur. Spine J. [Internet]. 28 (4), 658–664. https://doi.org/10.1007/s00586-018-5807-6.

Gandhi, A.A., Grosland, N.M., Kallemeyn, N.A., Kode, S., Fredericks, D.C., Smucker, J.D., 2019. Biomechanical analysis of the cervical spine following disc degeneration, disc

fusion, and disc replacement: a finite element study. Int. J. Spine Surg. 13 (6), 491–500.
Gore, D.R., Sepic, S.B., Gardner, G.M., 1986. Roentgenographic findings of the cervical spine in asymptomatic people. Spine (Phila Pa 1976) 11 (6), 521–524.
Guérin, P., Obeid, I., Gille, O., Bourghli, A., Luc, S., Pointillart, V., Vital, J.M., 2012. Sagittal alignment after single cervical disc arthroplasty. J. Spinal Disord. Tech. 25 (1), 10–16.
Heidsieck, C., Gajny, L., Travert, C., Lazennec, J.Y., Skalli, W., 2021. Effect of postural alignment alteration with age on vertebral strength. Osteoporos. Int. https://doi.org/10.1007/s00198-021-06093-0. In press.
Hogg-Johnson, S., van der Velde, G., Carroll, L.J., Holm, L.W., Cassidy, J.D., Guzman, J., Côté, P., Haldeman, S., Ammendolia, C., Carragee, E., et al., 2009. The burden and determinants of neck pain in the general population. results of the bone and joint decade 2000-2010 task force on neck pain and its associated disorders. J. Manipulative Physiol. Ther. 32 (2 SUPPL), 39–51.
Humbert, L., De Guise, J.A., Aubert, B., Godbout, B., Skalli, W., 2009. 3D reconstruction of the spine from biplanar X-rays using parametric models based on transversal and longitudinal inferences. Med. Eng. Phys. [Internet]. 31 (6), 681–687. https://doi.org/10.1016/j.medengphy.2009.01.003.
Hyun, S.J., Kim, K.J., Jahng, T.A., Kim, H.J., 2017. Clinical impact of T1 slope minus cervical lordosis after multilevel posterior cervical fusion surgery. Spine (Phila Pa 1976) 42 (24), 1859–1864.
John, J.D., Saravana Kumar, G., Yoganandan, N., 2019. Cervical spine morphology and ligament property variations: a finite element study of their influence on sagittal bending characteristics. J. Biomech. [Internet]. 85, 18–26. https://doi.org/10.1016/j.jbiomech.2018.12.044.
Katsuura, A., Hukuda, S., Saruhashi, Y., Mori, K., 2001. Kyphotic malalignment after anterior cervical fusion is one of the factors promoting the degenerative process in adjacent intervertebral levels. Eur. Spine J. 10 (4), 320–324.
Kim, S.W., Shin, J.H., Arbatin, J.J., Park, M.S., Chung, Y.K., McAfee, P.C., 2008. Effects of a cervical disc prosthesis on maintaining sagittal alignment of the functional spinal unit and overall sagittal balance of the cervical spine. Eur. Spine J. 17 (1), 20–29.
Klinich, K.D., Ebert, S., Van Ee, C., Flannagan, C., Prasad, M., Reed, M., Schneider, L., 2004. Cervical spine geometry in the automotive seated posture: Variations with age, stature, and gender. In: Proc 48th Stapp Car Crash Conf. [place unknown].
Kong, L., Cao, J., Wang, L., Shen, Y., 2016. Prevalence of adjacent segment disease following cervical spine surgery a PRISMA-compliant systematic review and meta-analysis. Medicine (Baltimore) 95 (27), e4171.
Lan, Z., Huang, Y., Xu, W., 2019. Relationship between T1 slope minus C2-7 lordosis and cervical alignment parameters after adjacent 2-level anterior cervical diskectomy and fusion of lower cervical spine. World Neurosurg. [Internet]. 122, e1195–e1201. https://doi.org/10.1016/j.wneu.2018.11.016.
Lau, K.T., Cheung, K.Y., Chan Kwok, B., Chan, M.H., Lo, K.Y., Wing Chiu, T.T., 2010. Relationships between sagittal postures of thoracic and cervical spine, presence of neck pain, neck pain severity and disability. Man. Ther. [Internet]. 15 (5), 457–462. https://doi.org/10.1016/j.math.2010.03.009.
Laville, A., Laporte, S., Skalli, W., 2009. Parametric and subject-specific finite element modelling of the lower cervical spine. Influence of geometrical parameters on the motion patterns. J. Biomech. 42 (10), 1409–1415.
Liu, J., Liu, P., Ma, Z., Mou, J., Wang, Z., Sun, D., Cheng, J., Zhang, D., Xiao, J., 2019. The effects of aging on the profile of the cervical spine. Med (United States). 98 (7), 1–5.
Mackiewicz, A., Banach, M., Denisiewicz, A., Bedzinski, R., 2016. Comparative studies of cervical spine anterior stabilization systems - finite element analysis. Clin. Biomech. [Internet]. 32, 72–79. https://doi.org/10.1016/j.clinbiomech.2015.11.016.
Marquez-Lara, A., Nandyala, S.V., Fineberg, S.J., Singh, K., 2014. Current trends in demographics, practice, and in-hospital outcomes in cervical spine surgery: A national database analysis between 2002 and 2011. Spine (Phila Pa 1976) 39 (6), 476–481.
Moroney, S.P., Schultz, A.B., Miller, J.A.A.A., 1988. Analysis and measurement of neck loads. J. Orthop. Res. 6 (5), 713–720.
Mortensen, J.D., Vasavada, A.N., Merryweather, A.S., 2018. The inclusion of hyoid muscles improve moment generating capacity and dynamic simulations in musculoskeletal models of the head and neck. PLoS One 13 (6), 1–14.
Murray, C., Atkinson, C., Bhalla, K., Birbeck, G., Burstein, R., Chou, D., 2013. The state of US health, 1990-2010: burden of diseases, injuries, and risk factors. JAMA - J. Am. Med. Assoc. [Internet]. 310 (6), 591–608. http://jama.jamanetwork.com/data/Journals/JAMA/927436/joi130037.pdf%5Cnhttp://ovidsp.ovid.com/ovidweb.cgi?T=JS&PAGE=reference&D=emed11&NEWS=N&AN=2013503627%5Cnhttp://ovidsp.ovid.com/ovidweb.cgi?T=JS&PAGE=reference&D=medl&NEWS=N&AN=23842577.
Nérot, A., Choisne, J., Amabile, C., Travert, C., Pillet, H., Wang, X., Skalli, W., 2015. A 3D reconstruction method of the body envelope from biplanar X-rays: evaluation of its accuracy and reliability. J. Biomech. [Internet]. 48 (16), 4322–4326. https://doi.org/10.1016/j.jbiomech.2015.10.044.
Nikkhoo, M., Cheng, C.H., Wang, J.L., Khoz, Z., El-Rich, M., Hebela, N., Khalaf, K., 2019. Development and validation of a geometrically personalized finite element model of the lower ligamentous cervical spine for clinical applications. Comput. Biol. Med. [Internet]. 109 (April), 22–32. https://doi.org/10.1016/j.compbiomed.2019.04.010.
Okada, E., Matsumoto, M., Ichihara, D., Chiba, K., Toyama, Y., Fujiwara, H., Momoshima, S., Nishiwaki, Y., Hashimoto, T., Ogawa, J., et al., 2009. Aging of the cervical spine in healthy volunteers: a 10-year longitudinal magnetic resonance imaging study. Spine (Phila Pa 1976) 34 (7), 706–712.
Rousseau, M.-A., Laporte, S., Chavary-Bernier, E., Lazennec, J.-Y.J.Y., Skalli, W., 2007. Reproducibility of measuring the shape and three-dimensional position of cervical vertebrae in upright position using the EOS stereoradiography system. Spine (Phila Pa 1976) 32 (23), 2569–2572.
Rousseau, M.-A., Bonnet, X., Skalli, W., 2008. Influence of the geometry of a ball-and-socket intervertebral prosthesis at the cervical spine: a finite element study. Spine (Phila Pa 1976) 33 (1), E10–E14.
Steffen, J.S., Obeid, I., Aurouer, N., Hauger, O., Vital, J.M., Dubousset, J., Skalli, W., 2010. 3D postural balance with regard to gravity line: an evaluation in the transversal plane on 93 patients and 23 asymptomatic volunteers. Eur. Spine J. 19 (5), 760–767.
Thenard, T., Vergari, C., Hernandez, T., Vialle, R., Skalli, W., 2019. Analysis of center of mass and gravity-induced vertebral axial torque on the scoliotic spine by barycentremetry. Spine Deform. 7 (4), 525–532.
Trinh, K., Graham, N., Gross, A., Ch, G., Wang, E., Id, C., Tm, K., 2006. Acupuncture for neck disorders (review). Cochrane Collab. 3, 1–41.
Van den Abbeele, M., Li, F., Pomero, V., Bonneau, D., Sandoz, B., Laporte, S., Skalli, W., 2018. A subject-specific biomechanical control model for the prediction of cervical spine muscle forces. Clin. Biomech. [Internet]. 51 (February), 58–66. https://doi.org/10.1016/j.clinbiomech.2017.12.001.
Vasavada, A.N., Nevins, D.D., Monda, S.M., Hughes, E., Lin, D.C., 2015. Gravitational demand on the neck musculature during tablet computer use. Ergonomics. 58 (6), 990–1004.
Wang, M.C., Kreuter, W., Wolfla, C.E., Maiman, D.J., Deyo, R.A., 2009. Trends and variations in cervical spine surgery in the United States: medicare beneficiaries, 1992 to 2005. Spine (Phila Pa 1976) 34 (9), 953–955.
Wang, X., Meng, Y., Liu, H., Chen, H., Wang, B., Hong, Y., 2021. Cervical sagittal alignment after prestige LP cervical disc replacement: radiological results and clinical impacts from a single-center experience. BMC Musculoskelet. Disord. 22 (1), 4–11.
Xiong, W., Zhou, J., Sun, C., Chen, Z., Guo, X., Huo, X., Liu, S., Li, J., Xue, Y., 2020. 0.5-to 1-fold intervertebral distraction is a protective factor for adjacent segment degeneration in single-level anterior cervical discectomy and fusion. Spine (Phila Pa 1976) 45 (2), 96–102.
Yoganandan, N., Pintar, F.A., Zhang, J., Baisden, J.L., 2009. Physical properties of the human head: mass, center of gravity and moment of inertia. J. Biomech. [Internet]. 42 (9), 1177–1192. https://doi.org/10.1016/j.jbiomech.2009.03.029.